

# Improved singlet oxygen generation in Rhenium(I) complexes functionalized with a pyridinyl selenoether ligand

Karina P. Morelli Frin<sup>1\*</sup>, Leonardo Henrique de Macedo<sup>1</sup>, Samuel Santos de Oliveira<sup>1</sup>,  
Rodrigo L.O. R. Cunha<sup>1</sup> and Jesus Calvo-Castro<sup>2</sup>

<sup>1</sup>Federal University of ABC - UFABC, Av. dos Estados 5001, Santo Andre-SP – Brazil -  
09210-170. [\\*karina.frin@ufabc.edu.br](mailto:*karina.frin@ufabc.edu.br)

<sup>2</sup>School of Life and Medical Sciences, University of Hertfordshire, Hatfield, AL10 9AB,  
U.K.

## Abstract

The synthesis, characterization, electrochemical and photophysical properties of three novel polypyridine rhenium(I) complexes coordinated to an organoselenide ligand, 4-(phenylseleno)-pyridine (PhSepy), and structurally related polypyridine ligands, *fac*-[Re(CO)<sub>3</sub>(NN)(PhSepy)]<sup>+</sup> NN = 1,10-phenanthroline (phen), 4,7-diphenyl-1,10-phenanthroline (ph<sub>2</sub>phen) and pyrazino[2,3-f]-1,10-phenanthroline (dpq), are reported. In addition, their ability to act as a photosensitizer agent for the generation of singlet oxygen was investigated. Cyclic and differential pulse voltammetry experiments showed an overlap of the redox waves characteristic of the 4-(phenylseleno)-pyridine ligand and the Re(I) complex. This finding is consistent with a strong contribution of the pyridine-based ligand on the HOMO levels of the three investigated complexes, further supported by quantum mechanical calculations. Moreover, the lowest energy band observed in the absorption spectra of the complexes was also influenced by the organoselenide ligand, with a combination of the usual MLCT<sub>Re→NN</sub> transition with a ligand-to-ligand charge transfer (LLCT) one. The three complexes showed typical emission spectra for this class of compounds ascribed to <sup>3</sup>MLCT<sub>Re→NN</sub>, with excellent quantum yields for the singlet oxygen generation ( $\Phi_{\Delta} = 0.65-0.70$ ). Remarkably, these are significantly larger (15-29%) than those for structurally related complexes with non-functionalized pyridyl ligands, revealing a significant ability as a photosensitizer agent. Therefore, we envisage this work to be of interest to those engaged in the development of novel rhenium(I) complexes for optoelectronic applications.

**Keywords:** Rhenium(I) compounds; organoselenide ligand;  $^3\text{MLCT}$  emission; singlet oxygen; photosensitizers.

## Introduction

The first study on rhenium polypyridine coordinated systems was reported by Wrighton and coworkers back in 1974 [1]. The reported photophysics has since fostered experimental [2-8] and theoretical [9-12] studies devoted to the in-depth evaluation of structure-property relationships in these complexes. Although there has been much discussion on these systems, there remains an acknowledged need to better understand their photophysical transitions to further pave the way for the realization of superior alternatives, which could be exploited in sensor and photocatalytic technologies as well as electroluminescent devices, among others.

It is nowadays well understood that the luminescence properties of the rhenium(I) complexes can be associated with the metal-to-ligand charge-transfer excited state, MLCT. These properties can be tailored by judicious substitution of the polypyridine ligands. In most cases, this can be achieved by i) modifying the ancillary ligand; and ii) introducing electron-donating/withdrawing groups on the diimine ligand [3, 13-21], which promotes the destabilization/stabilization of  $^3\text{MLCT}_{\text{Re} \rightarrow \text{NN}}$  excited state energy level, respectively.

The use of chalcogenide ligands coordinated to metal complexes has been reported in the literature for the last decades [22, 23]. Whilst a plethora of chalcogenides have been investigated to date, organoselenides, and in particular the selenoether moiety (C-Se-C) have been widely utilized [24]. In addition, the use of copper, palladium, and platinum with selenium ligands in coordination complexes has also been exploited [25, 26], having potential applications in the pharmacological and biochemical field [27], in catalysis [28], as well as more recently as phosphorescent emitters in light emitting diodes [29]. Selenium is an essential and unique trace element that plays a key role in a number of metabolic processes [30, 31] and exerts critical physiological functions mediated by its incorporation into selenoproteins, mainly in the form of selenocysteine, conferring an antioxidant character to these proteins [32]. However, Selenium typically turns into a pro-oxidant at elevated doses with well-established growth-inhibiting properties and

high cytotoxic activities, thereby exerting its potential anticancer properties [31-33]. The redox-properties of selenoether moieties and their antitumoral activity was advantageously associated to luminescent metal complexes towards the development of theranostic agents [34]. Despite the critical physiological function, selenium-bearing pyridine ligands have been scarcely utilized in rhenium(I) complexes [25, 35, 36].

Motivated by these findings, we went on in-depth evaluation of the effect of an organoselenide ligand in a series of three novel polypyridine (NN) rhenium-complexes. In particular, we explored 4-(phenylseleno)-pyridine (PhSepy) as the organoselenide ligand in Re(I) complexes bearing 1,10-phenanthroline (phen), 4,7-diphenyl-1,10-phenanthroline (ph<sub>2</sub>phen) and pyrazino[2,3-f]-1,10-phenanthroline (dpq) as the polypyridine ligands, *fac*-[Re(CO)<sub>3</sub>(NN)(PhSepy)]PF<sub>6</sub>, (Figure 1). To the best of our knowledge, this work denotes the first report of an organoselenide-pyridine ligand coordinated to rhenium(I) polypyridine complexes. These compounds were synthesized and characterized by <sup>1</sup>H NMR and IR spectroscopies as well as elemental analysis. Their electrochemical and photophysical properties were investigated as well as their ability to act as photosensitizing agents for the generation of singlet oxygen. It is of note that via careful peripheral substitutions, significantly greater (15-29%) singlet oxygen quantum efficiencies were observed for these three novel rhenium(I) complexes when compared to reported structural analogues not bearing the employed organoselenide ligand.

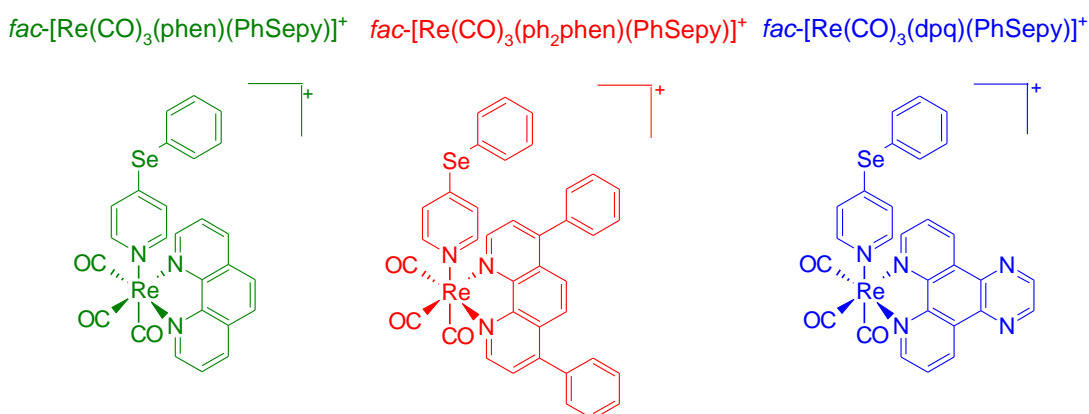


Figure 1. Chemical structures of rhenium(I) polypyridyl complexes based on 4-(phenylseleno)-pyridine.

## Experimental Section

## Materials

In all cases, reagent grade solvents were purchased from Aldrich or Synth and used without further purification. HPLC grade solvents were used for the photophysical and electrochemical characterization of the complexes reported, purchased from Aldrich or LIChrosolv, as received.

## Synthesis

### 4-(phenylseleno)-pyridine

The selenide compound was synthesized following the procedure previously reported [37, 38]. Diphenyl diselenide (3 mmol, 938 mg), (4-dihydroxiboro)-4-pyridine (6.6 mmol, 769 mg),  $\text{CuSO}_4$  (2.8 mmol, 446 mg), 1,10-phenanthroline monohydrate (2.8 mmol, 556 mg) and 75 mL of EtOH were placed in a reaction flask. After 2 min,  $\text{Na}_2\text{CO}_3$  (1.42 mmol, 150 mg) was added, and the mixture was stirred vigorously at room temperature for 22 h. At the end of the procedure, the EtOH was removed under reduced pressure and then extracted with EtOAc (20 mL), NaCl sat. (20mL). The crude product was purified on a flash silica gel column (hexane: ethyl acetate, 90:10). Yield 50% (702 mg).  $^1\text{H}$  NMR ( $\text{CD}_3\text{CN}$ , 500 MHz,  $\delta$  / ppm): 8.29 (d, 2H,  $J=6.11$  Hz); 7.67 (m, 2H); 7.47 (m, 3H); 7.16 (d, 2H,  $J = 6.11$  Hz).  $^{13}\text{C}$  NMR ( $\text{CDCl}_3$ , 50.33 MHz,  $\delta$  / ppm): 148.9, 145.3, 135.7, 129.4, 128.8, 125.6, 123.3.

### Rhenium(I) complexes

Rhenium(I) compounds were synthesized following the procedure previously reported [15, 16, 39-41]. Briefly, a small excess of NN ligand (1,10-phenanthroline (phen), 4,7-diphenyl-1,10-phenanthroline ( $\text{ph}_2\text{phen}$ ), pyrazino[2,3-f]-1,10-phenanthroline (dpq)) and  $[\text{ClRe}(\text{CO})_5]$  were mixed in xylene (Synth) and heated to reflux for 6 h. The hot mixture was separated by filtration. Then the correspondent *fac*- $[\text{ReCl}(\text{CO})_3(\text{NN})]$  was suspended to a 30 mL argon saturated dichloromethane, and after one hour, a 10-fold excess of trifluoromethanesulfonic acid (tfms) was added. The solution was stirred for one hour, and the resulting product, *fac*- $[\text{Re}(\text{tfms})(\text{CO})_3(\text{NN})]$ , was obtained by slow addition of ethyl ether. Lastly, in a 30 mL of argon saturated solution of *fac*- $[\text{Re}(\text{tfms})(\text{CO})_3(\text{NN})]$  complex was added to a small excess of 4-(phenylseleno)-pyridine (PhSepy) and heated to reflux under an argon atmosphere for 6 hours. After cooling to

room temperature, the final product was precipitated by the addition of solid  $\text{NH}_4\text{PF}_6$ . The yellow solid was separated by filtration, washed with water and ethyl ether.

For *fac*- $[\text{Re}(\text{CO})_3(\text{phen})(\text{PhSepy})]\text{PF}_6$  the yield was 80% (500 mg). Anal. Calc. for  $\text{C}_{26}\text{H}_{17}\text{N}_3\text{F}_6\text{O}_3\text{PReSe}$ : C, 37.64%; H, 2.07%; N, 5.07%; Found: C, 37.30%; H, 1.93%; N, 5.12%. ( $\text{CD}_3\text{CN}$ , 500 MHz,  $\delta$  / ppm): 9.53 (dd, 2H,  $J = 5.14$ ; 1.22 Hz); 8.82 (dd, 2H,  $J = 8.32$ ; 1.22 Hz); 8.16 (s, 2H); 8.07 (dd, 2H,  $J = 8.32$ ; 5.14 Hz); 7.85 (d, 2H,  $J = 6.85$  Hz); 7.50 (m, 3H); 7.41 (m, 2H); 6.86 (d, 2H,  $J = 6.85$  Hz).

For *fac*- $[\text{Re}(\text{CO})_3(\text{ph}_2\text{phen})(\text{PhSepy})]\text{PF}_6$  the yield was 34% (110 mg). Anal. Calc. for  $\text{C}_{38}\text{H}_{25}\text{N}_3\text{F}_6\text{O}_3\text{PReSe}$ : C, 46.49%; H, 2.57%; N, 4.28%; Found: C, 46.09%, H, 2.33%; N, 4.01%. ( $\text{CD}_3\text{CN}$ , 500 MHz,  $\delta$  / ppm): 9.56 (d, 2H,  $J = 5.38$  Hz); 8.09 (s, 2H); 8.01 (d, 2H,  $J = 5.38$  Hz); 7.94 (d, 2H,  $J = 6.85$  Hz); 7.63 (m, 10H); 7.52 (m, 3H); 7.43 (m, 2H); 6.94 (d, 2H,  $J = 6.85$  Hz).

For *fac*- $[\text{Re}(\text{CO})_3(\text{dpq})(\text{PhSepy})]\text{PF}_6$  the yield was 43% (350 mg). Anal. Calc. for  $\text{C}_{28}\text{H}_{17}\text{N}_5\text{F}_6\text{O}_3\text{PReSe}$ : C, 38.15%; H, 1.94%; N, 7.94%; Found: C, 38.39%; H, 2.18%; N, 8.05%. ( $\text{CD}_3\text{CN}$ , 500 MHz,  $\delta$  / ppm): 9.77 (dd, 2H,  $J = 8.24$ ; 1.22 Hz); 9.61 (dd, 2H,  $J = 5.19$ ; 1.22 Hz); 9.21 (s, 2H); 8.22 (dd, 2H,  $J = 8.24$ ; 5.19 Hz); 7.88 (dd, 2H,  $J = 7.02$  Hz); 7.48 (m, 3H); 7.40 (m, 2H); 6.88 (d, 2H,  $J = 7.02$  Hz).

## Methods

Proton nuclear magnetic resonance spectra ( $^1\text{H}$  NMR) were obtained on a Bruker Avance III (500 MHz) spectrometer at 298 K using an appropriated deuterated solvent, and their residual signals were employed as the internal standard. Absorption spectra were recorded on an Agilent 8453 spectrophotometer using a 1.00 cm optical length quartz cuvette. The Fourier-transformed infrared (FT-IR) spectra of all compounds were recorded by attenuated total reflectance (ATR) with a Spectrum Two Spectrometer, Perkin Elmer, and collected for 16 scans at  $2\text{ cm}^{-1}$  resolution.

The cyclic and differential pulse voltammetry experiments were performed in a potentiostat/galvanostat  $\mu$ autolab type III model (Autolab, The Netherlands). The set of electrodes used during the electrochemical procedure were: glassy carbon as the working electrode; platinum as the counter electrode; and  $\text{Ag}/\text{Ag}^+$  as the reference electrode. All the measurements were carried out in deaerated acetonitrile solution

containing the rhenium(I) complex (1 mM) or the free PhSepy compound (1 mM) and tetrabutylammonium hexafluorophosphate (0.1 M) as the supporting electrolyte at a scan rate of 100 mV s<sup>-1</sup>. The potential measurements were recorded vs. Ag/Ag<sup>+</sup> and the internal standard Fc<sup>+</sup>/Fc couple, and then converted to E<sub>1/2</sub> versus the normal hydrogen electrode (NHE) using E<sub>1/2(Fc+/Fc)</sub> = +0.69 V versus NHE [42].

Computational details: relaxed ground-state geometries of the three investigated complexes were optimized by means of the B3LYP density functional [43-45] with the D3 parametrization of Grimme [46] and triple-zeta basis set including diffusion effects on heavy atoms and polarization effects on all atoms [47], as implemented in Spartan '18, v.1.4.4 [48]. In all cases, energy minima were confirmed by IR analysis [49], which were characterized by the absence of any imaginary modes, thus consistent with real equilibrium minima. Franck-Condon transitions were computed in acetonitrile, using the polarizable continuum model [50], within the framework of TD-DFT [51, 52] and the Tamm-Dancoff approximation [53], employing the same density functional and level described before.

Emission spectra at room temperature (298 K) were recorded with a Varian Cary Eclipse steady-state spectrophotometer using a 1.00 cm optical length quartz cuvette for the fluid solution. The spectra were not corrected for the photomultiplier spectral response in the 700 – 750 nm region. Emission quantum yields of rhenium(I) compounds were determined employing a relative method [54, 55] using *fac*-[Re(CO)<sub>3</sub>(phen)(py)]<sup>+</sup>, py = pyridine, as the standard (0.18 in CH<sub>3</sub>CN, 298 K [56]). Diluted solutions (~10<sup>-5</sup> M; optical densities below 0.2 in all cases at excitation wavelength – 375 nm) of the standard and the samples were prepared to minimize the possibility of aggregation and were degassed with argon for 30 min, and then the emission spectra were recorded using the same setup condition for the sample and the standard. Phosphorescence decay times were obtained by a time-correlated single-photon counting (TCSPC) setup (FluoTime 300, Picoquant GmbH) using as an excitation source a 375 nm diode laser (LDH-P-375B, 40 MHz repetition rate, 52 ps pulse width, PicoQuant GmbH) driven by PDL 820 computer controller. The emission wavelengths were isolated using a monochromator, and solutions were characterized by optical densities below 0.2 in all cases and were degassed for 30 min using an argon atmosphere. The generation of singlet oxygen was

monitored at 1270 nm using a Hamamatsu Near Infrared (NIR) photomultiplier. The solutions were air equilibrated and the quantum yields were determined at room temperature, as already described, using  $[\text{Ru}(\text{bpy})_3]^{2+}$  ( $\Phi_{\Delta}^S = 0.56$  in  $\text{CH}_3\text{CN}$  [57, 58]) and/or *fac*- $[\text{Re}(\text{CO})_3(\text{phen})(\text{py})]^+$  ( $\Phi_{\Delta}^S = 0.59$  in  $\text{CH}_3\text{CN}$  [56]) as the standard.

## Results and Discussion

The three novel reported Re(I) complexes were synthesized and subsequently characterized by FT-IR and  $^1\text{H}$  NMR spectroscopies (Figures S1-S5) as well as elemental analysis. Fourier-transformed infrared (FT-IR) spectra of these three novel complexes, illustrated in Figure 2, are consistent with the expected spectral profile for rhenium(I) complexes with the presence of intense bands around  $2100\text{-}1800\text{ cm}^{-1}$  ascribed to the C-O stretching vibration characteristic of a facial geometry [3, 59-61]. The high intensity IR-active vibrational band at ca.  $830\text{ cm}^{-1}$  can be ascribed to the counter ion  $\text{PF}_6^-$  [17, 59, 62], and additional bands in the  $1800 - 500\text{ cm}^{-1}$  region were also observed and identified as ring vibrations of the coordinated ligands [63]. These key IR-active carbonyl stretching vibrations are associated with equatorial and ancillary substitutions and are further confirmed by computational approaches for optimized geometries of these complexes (Tables S1-S5).

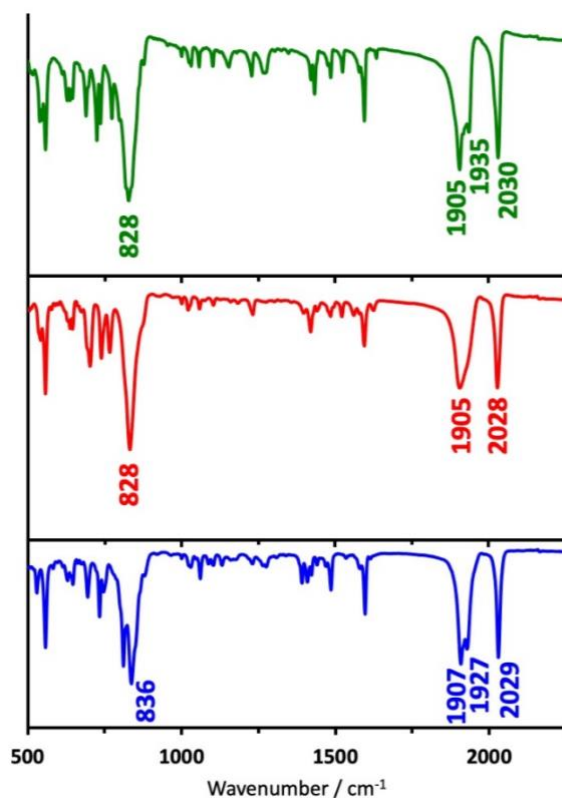


Figure 2. FT-IR spectra of *fac*-[Re(CO)<sub>3</sub>(NN)(PhSepy)]PF<sub>6</sub>, NN = phen (green solid line), ph<sub>2</sub>phen (red solid line) and dpq (blue solid line).

Next, we went on to investigate the electrochemical properties of these Re(I) complexes using differential pulse (DPV) and cyclic voltammetry (CV). Figure 3 illustrates the differential pulse voltammograms for these metal complexes as well as the 4-(phenylseleno)-pyridine ligand for comparison (Figure S6).

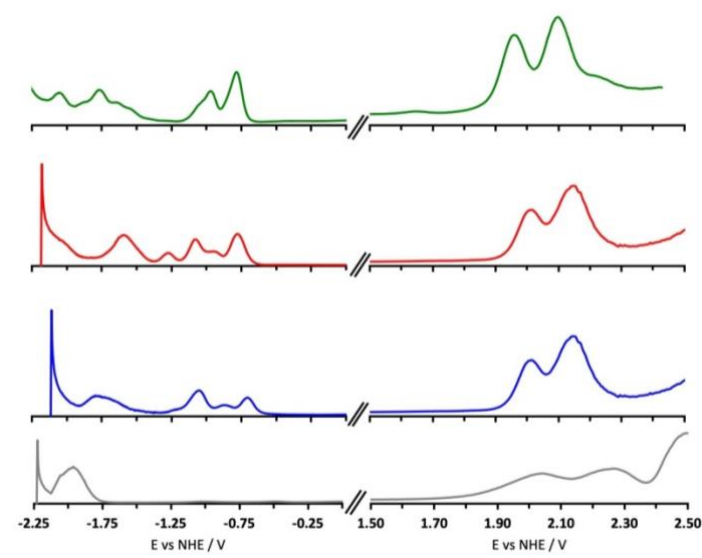


Figure 3. Differential pulse voltammograms of *fac*-[Re(CO)<sub>3</sub>(phen)(PhSepy)]<sup>+</sup> (green solid line), *fac*-[Re(CO)<sub>3</sub>(ph<sub>2</sub>phen)(PhSepy)]<sup>+</sup> (red solid line) *fac*-[Re(CO)<sub>3</sub>(dpq)(PhSepy)]<sup>+</sup> (blue solid line) and free PhSepy for comparison (grey solid line) in acetonitrile. Scan rate of 100 mV s<sup>-1</sup>.

It has been widely reported that rhenium(I) complexes are characterized by oxidation and reduction processes associated with the metal ion Re<sup>I/II</sup> and the polypyridine ligand [NN→NN\*], respectively [1, 13, 14, 16]. For the compounds investigated herein, the reduction process of the polypyridine ligands is clearly observed between -1.5 and -0.5 V vs. NHE. On the other hand, the oxidation process of Re<sup>I</sup> to Re<sup>II</sup>, which typically occurs at potential from 1.0-2.0 V vs. NHE [14, 16], is close to the observed potential for oxidation of the PhSepy ligand (grey solid line), with the latter precluding the accurate determination of the Re(I) oxidation in these *fac*-[Re(CO)<sub>3</sub>(NN)(PhSepy)]<sup>+</sup> complexes. On comparing our findings to those previously reported for py-bearing Re(I) complexes [14], we hypothesized greater contribution of the PhSepy ligand on the highest occupied molecular orbital (HOMO) wavefunction in these systems based on electrochemical data (Figure 3). In fact, frontier molecular orbital wavefunctions for the optimized geometries of these Re(I) complexes (Figure 4, Table S6) are consistent with these findings. In essence, whilst we observe strong contributions from the PhSepy ligand on the HOMO surfaces, the opposite was observed for the phenanthroline substitutions.

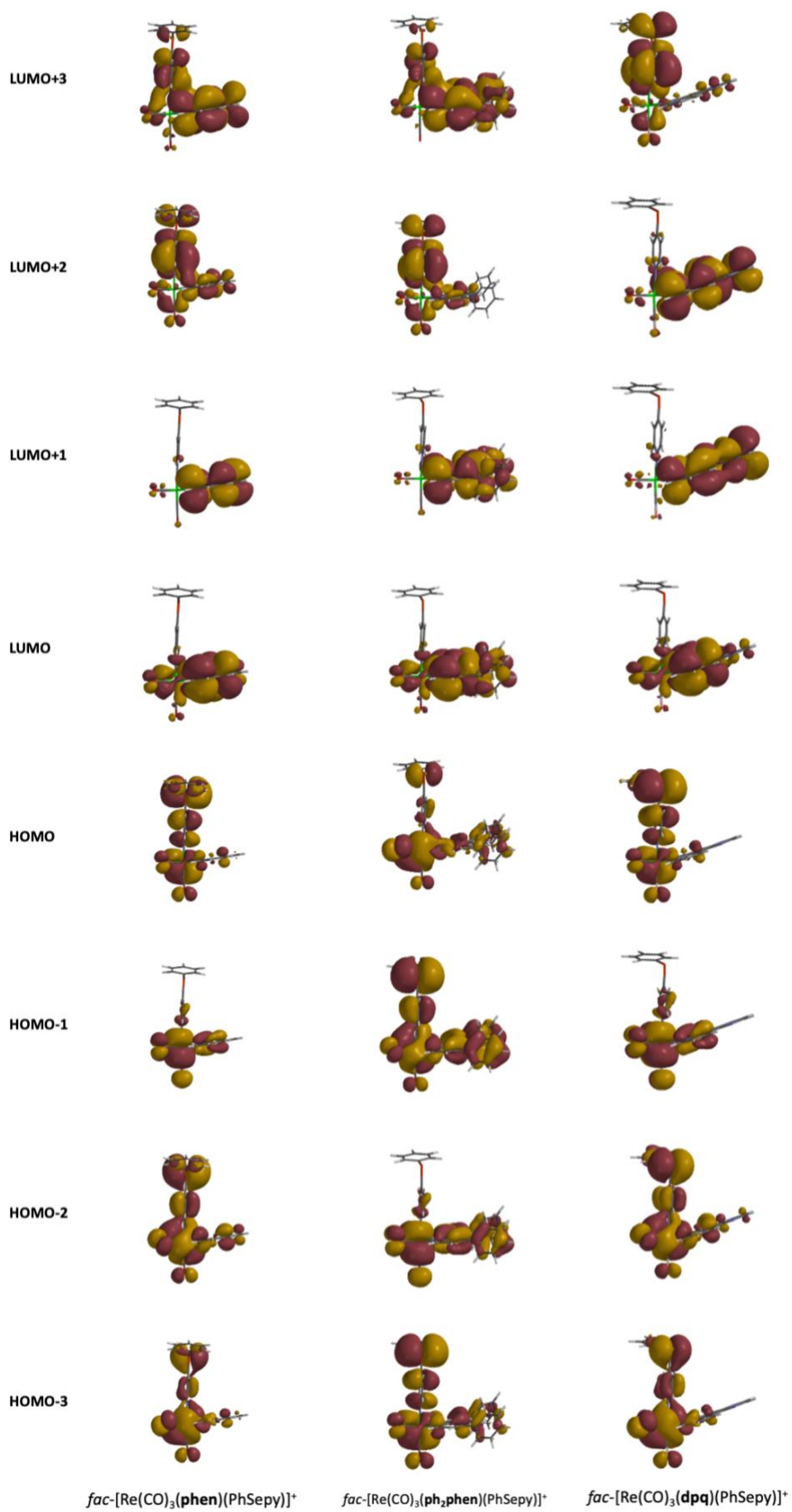


Figure 4. Illustration of key molecular orbitals of *fac*-[Re(CO)<sub>3</sub>(phen)(PhSepy)]PF<sub>6</sub>, *fac*-[Re(CO)<sub>3</sub>(ph<sub>2</sub>phen)(PhSepy)]PF<sub>6</sub> and *fac*-[Re(CO)<sub>3</sub>(dpq)(PhSepy)]PF<sub>6</sub> optimized at B3LYP-D3/6-311+G(d)(p). IsoVal = 0.01.

Figure 5 illustrates the absorption spectra of *fac*-[Re(CO)<sub>3</sub>(NN)(PhSepy)]<sup>+</sup> complexes in acetonitrile along with the spectrum of the PhSepy ligand for comparison. In all cases, we report strong absorptions in the high energy spectral region ranging from 200-300 nm, which can be associated with polypyridyl intraligand electronic transitions,  $IL_{NN}$ . The inflections on the red end of these bands, at ca. 370 nm, can be ascribed to metal-to-ligand charge transfer transitions,  $MLCT_{Re \rightarrow NN}$ . These are consistent with previously reported observations for structurally related Re(I) complexes [13-15, 19]. Vertical electronic transitions were further evaluated through TD-DFT calculations on optimized geometries of these Re(I) complexes (Tables S7-S9). In short, computed vertical transitions were observed to account well for the experimental observations. In this regard, significantly larger oscillator strength was computed for the lowest energy transition of the ph<sub>2</sub>phen-bearing complex ( $f = 0.110$ ) when compared to that in the structural analogues ( $f = 0.056$  and  $0.044$  for phen- and dpq-bearing Re(I) complexes, respectively) which is in agreement with the experimentally observed hyperchromic shift for this absorption band (Figure 5). Additionally, the lowest energy transitions for all three complexes were observed to be HOMO→LUMO in character (Figure 4 and Tables S7-S9). We report in all cases, HOMO surfaces that primarily localize on the metal center as well as the PhSepy ligand. In turn, preferential localization of the density for the LUMO is observed on the metal-center and polypyridine ligand. As a result, the nature of the lowest energy electronic transition is characterized by a combination of  $MLCT_{Re \rightarrow NN}$  and LLCT (Ligand to Ligand Charge Transfer) transitions.

The comparison between the spectra of pyridine and pyridine-substituted compounds, such as *fac*-[Re(CO)<sub>3</sub>(NN)(py)]<sup>+</sup> [14] or *fac*-[Re(CO)<sub>3</sub>(NN)(bpa)]<sup>+</sup> [15, 64], shows that the incorporation of 4-(phenylseleno) moiety at the pyridine ring promotes a significant change on the absorption profile. The influence of the intraligand transition of the PhSepy ligand ( $\pi \rightarrow \pi^*$ , Se (4p)  $n \rightarrow \pi^*$ ) can be seen through the band centered at ca. 300 nm [65].

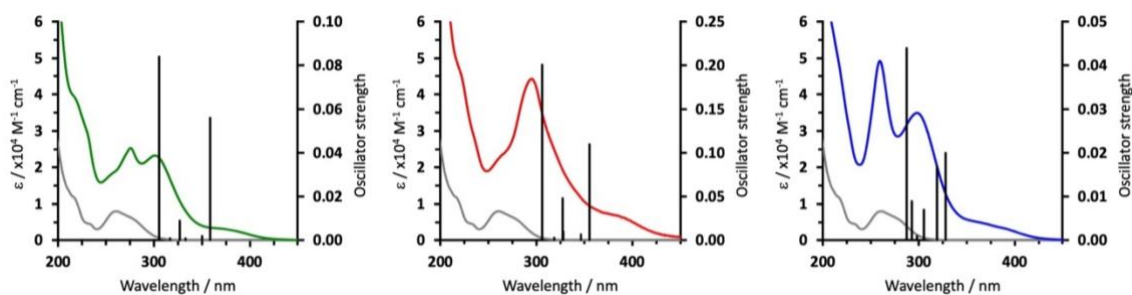


Figure 5. Absorption spectra of  $fac$ -[Re(CO)<sub>3</sub>(NN)(PhSepy)]<sup>+</sup>, NN = phen (green solid line), ph<sub>2</sub>phen (red solid line) and dpq (blue solid line), and the free PhSepy ligand for comparison (grey solid line) in acetonitrile at room temperature (298 K). Vertical black solid lines illustrate computed and corrected singlet vertical transitions, in acetonitrile, for the optimized geometries at B3LYP-D3/6-311+G(d)(p) (See Tables S7-9 for more details).

We observed arguably small changes in the phosphorescence emission of the metal complexes upon substitution on the phenanthroline moieties, with emission maximum ranging from 550-567 nm, as illustrated in Figure 6. Their photoluminescence quantum yields, denoting a key parameter in the development of singlet oxygen photosensitizers, were experimentally determined by a relative method. Importantly, the three investigated compounds are characterized by low photoluminescence quantum yields in degassed acetonitrile solutions, Table 1.

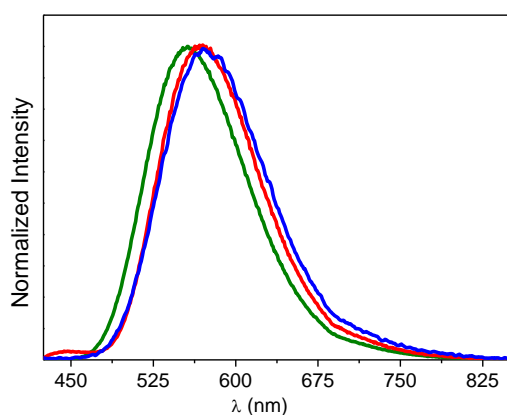


Figure 6. Emission spectra of  $fac$ -[Re(CO)<sub>3</sub>(NN)(PhSepy)]<sup>+</sup>, NN = phen (green solid line), ph<sub>2</sub>phen (red solid line) and dpq (blue solid line), in CH<sub>3</sub>CN at 298 K. ( $\lambda_{exc}$  = 375 nm)

Table 1. Emission data for rhenium(I) compounds in acetonitrile at 298 K.

Compound	$\lambda_{\text{max}}^{\text{em}}$ (nm)	$\phi$	$\tau$ ( $\mu\text{s}$ )	$k_r$ ( $\times 10^5 \text{ s}^{-1}$ )	$k_{\text{nr}}$ ( $\times 10^5 \text{ s}^{-1}$ )
<i>fac</i> -[Re(CO) <sub>3</sub> (phen)(PhSepy)] <sup>+</sup>	557	0.145 ± 0.004	0.88 ± 0.01	1.65	9.71
<i>fac</i> -[Re(CO) <sub>3</sub> (ph <sub>2</sub> phen)(PhSepy)] <sup>+</sup>	567	0.124 ± 0.009	1.90 ± 0.02	0.65	4.61
<i>fac</i> -[Re(CO) <sub>3</sub> (dpq)(PhSepy)] <sup>+</sup>	571	0.049 ± 0.005	0.40 ± 0.01	1.2	23.7
<i>fac</i> -[Re(CO) <sub>3</sub> (phen)(py)] <sup>+</sup> [56]	550	0.179 ± 0.004	1.30	1.38	6.32
<i>fac</i> -[Re(CO) <sub>3</sub> (ph <sub>2</sub> phen)(py)] <sup>+</sup>	563	0.203 ± 0.003	1.47 ± 0.01	1.38	5.4
<i>fac</i> -[Re(CO) <sub>3</sub> (dpq)(py)] <sup>+</sup> [66]	565	0.057	0.45	1.27	20.9

The *fac*-[Re(CO)<sub>3</sub>(NN)(PhSepy)]<sup>+</sup> compounds displayed broad emission spectra in acetonitrile, and the time-resolved decay curves are consistent with single exponential decay (Figures S7 – S9). Thus, this broad and non-structured emission can be assigned to be arising from the lowest-lying excited state <sup>3</sup>MLCT, typical of the rhenium(I) complexes [13, 14, 16, 19, 61]. Increasing emission energy is expected to result in higher emission quantum yields and longer emission lifetimes [67]. We observed that whilst two out of the three materials herein reported obeyed the energy gap law, this was not the case for the complex with ph<sub>2</sub>phen. This observation is unusual for pure MLCT emission, indicating the presence of another closer lying excited state, which also contributes to dissipate the energy.

Additionally, the substitution of the phen ligand by the dpq causes a small bathochromic shift in the emission band, along with a much lower emission quantum yield for the latter substitution. Similarly to the case observed for structural analogues *fac*-[Re(CO)<sub>3</sub>(NN)(bpa)]<sup>+</sup> (NN = phen and dpq, bpa = 1,2-bis(4-pyridyl)ethane) [15], these findings could be attributed to the non-emissive metal to the pyrazine moiety of the dpq ligand (<sup>3</sup>MLCT<sub>pz</sub>) excited state, which contributed to the deactivation manifold.

Lastly, we devote the remaining of this work to the investigation of the ability of these Re(I) complexes to be employed as singlet oxygen photosensitizers, following a

previously reported method [56]. Singlet oxygen quantum yields for *fac*-[Re(CO)<sub>3</sub>(NN)(PhSepy)]<sup>+</sup> complexes are summarized in Table 2.

Table 2. Singlet oxygen quantum yields for *fac*-[Re(CO)<sub>3</sub>(NN)(PhSepy)]<sup>+</sup> complexes in acetonitrile solution.

Compound	$\Phi_{\Delta}$
<i>fac</i> -[Re(CO) <sub>3</sub> (phen)(PhSepy)] <sup>+</sup>	0.69±0.01
<i>fac</i> -[Re(CO) <sub>3</sub> (ph <sub>2</sub> phen)(PhSepy)] <sup>+</sup>	0.70±0.01
<i>fac</i> -[Re(CO) <sub>3</sub> (dpq)(PhSepy)] <sup>+</sup>	0.65±0.01

In a degassed solution, an emission from this excited state can be observed with satisfactory quantum yields and long lifetimes (Table 1). On the other hand, in the presence of air-equilibrated solution, the energy is transferred from the triplet MLCT excited state of rhenium complexes to oxygen. In all cases, we report large quantum yields for singlet oxygen generation (Table 2), particularly in the cases of phen and ph<sub>2</sub>phen substituted rhenium(I) complexes. Interestingly, when compared to structurally-related photosensitizers previously reported, we observe a significant increase in  $\Phi_{\Delta}$  associated to the presence of the PhSepy ligand exploited in this work ( $\Phi_{\Delta} = 0.59 \pm 0.02$  for *fac*-[Re(CO)<sub>3</sub>(phen)(py)]<sup>+</sup>,  $\Phi_{\Delta} = 0.42 \pm 0.07$  for *fac*-[Re(CO)<sub>3</sub>(phen)(ampy)]<sup>+</sup> [56] and  $\Phi_{\Delta} = 0.50 \pm 0.05$  for *fac*-[Re(CO)<sub>3</sub>(ph<sub>2</sub>phen)(ampy)]<sup>+</sup> (ampy = 2-aminomethylpyridine) [19] in CH<sub>3</sub>CN). As a result, we have demonstrated that the incorporation of the 4-(phenylseleno) moiety in rhenium(I) complexes significantly contributes to the increase of singlet oxygen photogeneration and can serve as a blueprint for the subsequent development of superior alternative phototoxic agents.

## Conclusion

In this contribution, we report on the photophysical properties of rhenium(I) complexes by exploiting a novel coordinated ligand, 4-(phenylseleno)-pyridine (PhSepy) in a series

of structurally related polypyridine ligands (NN). These *fac*-[Re(CO)<sub>3</sub>(NN)(PhSepy)]<sup>+</sup> complexes (NN = phen, ph<sub>2</sub>phen, and dpq) were synthesized, characterized, and their electrochemical and photophysical properties were investigated. We observed that the coordination of an organoselenide ligand has a strong influence on the HOMO levels of the complexes, exemplified by an overlap of the redox waves of the PhSepy ligand and the Re(I) complex, and a combination of the usual MLCT<sub>Re→NN</sub> transition with a Ligand-to-ligand charge transfer (LLCT) in the lowest energy electronic transition. This behavior is not observed for the analogous pyridine complexes and hence can serve as a blueprint for the rational design of Re(I) complexes bearing such ligand motifs. The broad and non-structured emission band for the three complexes is ascribed to the lowest-lying <sup>3</sup>MLCT<sub>Re→NN</sub> excited state, typical of rhenium(I) polypyridine complexes. On the other hand, the complexes investigated herein exhibited remarkable quantum yields for the generation of the singlet oxygen, in contrast to the analogous pyridine complexes resulting in an increase of 15-29% in the <sup>1</sup>O<sub>2</sub> generation quantum yields. Overall, our findings contribute to the design of new complexes for optoelectronic applications and broaden the applications of selenoether compounds.

### **Acknowledgments**

The authors would like to acknowledge financial support from Fundação de Amparo a Pesquisa do Estado de São Paulo [FAPESP/Grant 2017/18063-0], UFABC's Strategic Research Units NBB and NuTS, and National System of Nanotechnology Laboratories - SisNANO, Proc. CNPq 402289/2013-7. Central Experimental Multiusuário (CEM-UFABC) and the Complexo Laboratorial Nanotecnológico (CLN-UFABC) are acknowledged for experimental support.

### **Supporting Information**

NMR spectra, Geometry optimization parameters, DFT structures, Cyclic voltammograms, Time-resolved decay curves.

## Notes

The authors declare no competing financial interest.

## References

- [1] M. Wrighton, D.L. Morse, *J. Am. Chem. Soc.* 96 (1974) 998-1003.
- [2] S.S. Sun, A.J. Lees, *Coord. Chem. Rev.* 230 (2002) 171-192.
- [3] A.S. Polo, M.K. Itokazu, N.Y. Murakami Iha, *J. Photochem. Photobiol., A* 181 (2006) 73-78.
- [4] H. Takeda, K. Koike, T. Morimoto, H. Inumaru, O. Ishitani, *Adv. Inorg. Chem.* 63 (2011) 137-186.
- [5] A.V. Müller, M.R. Gonçalves, L.D. Ramos, A.S. Polo, K.P.M. Frin, *Quim. Nova* 40 (2017) 200-213.
- [6] J. Rohacova, O. Ishitani, *Dalton Trans.* 46 (2017) 8899-8919.
- [7] K.K.-W. Lo, *Acc. Chem. Res.* 53 (2020) 32-44.
- [8] E. Wolcan, *Inorg. Chim. Acta* 509 (2020) 119650.
- [9] D.J. Stufkens, A. Vlček, *Coord. Chem. Rev.* 177 (1998) 127-179.
- [10] M. Kayanuma, C. Daniel, H. Köppel, E. Gindensperger, *Coord. Chem. Rev.* 255 (2011) 2693-2703.
- [11] C. Daniel, *Coord. Chem. Rev.* 282-283 (2015) 19-32.
- [12] J. Eng, C. Gourlaouen, E. Gindensperger, C. Daniel, *Acc. Chem. Res.* 48 (2015) 809-817.
- [13] L. Sacksteder, A.P. Zipp, E.A. Brown, J. Streich, J.N. Demas, B.A. DeGraff, *Inorg. Chem.* 29 (1990) 4335-4340.
- [14] L. Wallace, D.P. Rillema, *Inorg. Chem.* 32 (1993) 3836-3843.
- [15] S.F. Sousa, R.N. Sampaio, N.M. Barbosa Neto, A.E.H. Machado, A.O.T. Patrocinio, *Photochemical & Photobiological Sciences* 13 (2014) 1213-1224.
- [16] M.R. Gonçalves, K.P.M. Frin, *Polyhedron* 97 (2015) 112-117.
- [17] L.D. Ramos, R.N. Sampaio, F.F. de Assis, K.T. de Oliveira, P. Homem-de-Mello, A.O.T. Patrocinio, K.P.M. Frin, *Dalton Trans.* 45 (2016) 11688-11698.
- [18] R.C. Evans, P. Douglas, C.J. Winscom, *Coord. Chem. Rev.* 250 (2006) 2093-2126.
- [19] L.D. Ramos, G. Cerchiaro, K.P. Morelli Frin, *Inorg. Chim. Acta* 501 (2020) 119329.
- [20] B.L. Souza, L.A. Faustino, F.S. Prado, R.N. Sampaio, P.I.S. Maia, A.E.H. Machado, A.O.T. Patrocinio, *Dalton Trans.* (2020).
- [21] L.D. Ramos, L.H. de Macedo, N.R.S. Gobo, K.T. de Oliveira, G. Cerchiaro, K.P. Morelli Frin, *Dalton Trans.* (2020).
- [22] E.W. Abel, S.K. Bhargava, K.G. Orrell, *The Stereodynamics of Metal Complexes of Sulfur-, Selenium-, and Tellurium-Containing Ligands*, in: *Prog. Inorg. Chem.*, 1984, pp. 1-118.
- [23] W. Levason, S.D. Orchard, G. Reid, *Coord. Chem. Rev.* 225 (2002) 159-199.
- [24] A. Kumar, G.K. Rao, F. Saleem, A.K. Singh, *Dalton Trans.* 41 (2012) 11949-11977.
- [25] R. Cargnelutti, R.F. Schumacher, A.L. Belladonna, J.C. Kazmierczak, *Coord. Chem. Rev.* 426 (2021) 213537.
- [26] G. Kedarnath, V.K. Jain, *Coord. Chem. Rev.* 257 (2013) 1409-1435.
- [27] A. Kamal, M.A. Iqbal, H.N. Bhatti, *Reviews in Inorganic Chemistry* 38 (2018) 49-76.
- [28] A. Arora, S. Singh, P. Oswal, D. Nautiyal, G.K. Rao, S. Kumar, A. Kumar, *Coord. Chem. Rev.* 438 (2021) 213885.

- [29] P. Arsenyan, A. Petrenko, K. Leitonas, D. Volyniuk, J. Simokaitiene, T. Klinavičius, E. Skuodis, J.-H. Lee, J.V. Gražulevičius, *Inorg. Chem.* 58 (2019) 10174-10183.
- [30] C. Sanmartin, D. Plano, J.A. Palop, *Mini Reviews in Medicinal Chemistry* 8 (2008) 1020-1031.
- [31] A.P. Fernandes, V. Gandin, *Biochimica et Biophysica Acta (BBA) - General Subjects* 1850 (2015) 1642-1660.
- [32] G.N. Schrauzer, *Crit. Rev. Biotechnol.* 29 (2009) 10-17.
- [33] Z. Chen, H. Lai, L. Hou, T. Chen, *Chem. Commun.* 56 (2020) 179-196.
- [34] Z. Zhao, P. Gao, Y. You, T. Chen, *Chem. Eur. J.* 24 (2018) 3289-3298.
- [35] B. Manimaran, A. Vanitha, M. Karthikeyan, B. Ramakrishna, S.M. Mobin, *Organometallics* 33 (2014) 465-472.
- [36] A. Meltzer, R. Cargnelutti, A. Hagenbach, E. Schulz Lang, U. Abram, Z. *Anorg. Allg. Chem.* 641 (2015) 2617-2623.
- [37] N. Taniguchi, *The Journal of Organic Chemistry* 72 (2007) 1241-1245.
- [38] B. Zheng, Y. Gong, H.-J. Xu, *Tetrahedron* 69 (2013) 5342-5347.
- [39] K.P.M. Frin, N.Y. Murakami Iha, *Inorg. Chim. Acta* 376 (2011) 531-537.
- [40] K.P.M. Frin, R.M. de Almeida, *Photochemical & Photobiological Sciences* 16 (2017) 1230-1237.
- [41] K.M. Frin, N.Y.M. Iha, *J. Braz. Chem. Soc.* 17 (2006) 1664-1671.
- [42] V.V. Pavlishchuk, A.W. Addison, *Inorg. Chim. Acta* 298 (2000) 97-102.
- [43] A.D. Becke, *Physical Review A* 38 (1988) 3098-3100.
- [44] C. Lee, W. Yang, R.G. Parr, *Physical Review B* 37 (1988) 785-789.
- [45] A.D. Becke, *The Journal of Chemical Physics* 98 (1993) 5648-5652.
- [46] S. Grimme, J. Antony, S. Ehrlich, H. Krieg, *The Journal of Chemical Physics* 132 (2010) 154104.
- [47] E. Van Lenthe, E.J. Baerends, *J. Comput. Chem.* 24 (2003) 1142-1156.
- [48] Y. Shao, L.F. Molnar, Y. Jung, J. Kussmann, C. Ochsenfeld, S.T. Brown, A.T.B. Gilbert, L.V. Slipchenko, S.V. Levchenko, D.P. O'Neill, R.A. DiStasio Jr, R.C. Lochan, T. Wang, G.J.O. Beran, N.A. Besley, J.M. Herbert, C. Yeh Lin, T. Van Voorhis, S. Hung Chien, A. Sodt, R.P. Steele, V.A. Rassolov, P.E. Maslen, P.P. Korambath, R.D. Adamson, B. Austin, J. Baker, E.F.C. Byrd, H. Dachsel, R.J. Doerksen, A. Dreuw, B.D. Dunietz, A.D. Dutoi, T.R. Furlani, S.R. Gwaltney, A. Heyden, S. Hirata, C.-P. Hsu, G. Kedziora, R.Z. Khalliulin, P. Klunzinger, A.M. Lee, M.S. Lee, W. Liang, I. Lotan, N. Nair, B. Peters, E.I. Proynov, P.A. Pieniazek, Y. Min Rhee, J. Ritchie, E. Rosta, C. David Sherrill, A.C. Simmonett, J.E. Subotnik, H. Lee Woodcock Iii, W. Zhang, A.T. Bell, A.K. Chakraborty, D.M. Chipman, F.J. Keil, A. Warshel, W.J. Hehre, H.F. Schaefer Iii, J. Kong, A.I. Krylov, P.M.W. Gill, M. Head-Gordon, *PCCP* 8 (2006) 3172-3191.
- [49] F. Jensen, *Introduction to Computational Chemistry*, 3rd Edition ed., John Wiley and Sons, 2017.
- [50] E. Cancès, B. Mennucci, J. Tomasi, *The Journal of Chemical Physics* 107 (1997) 3032-3041.
- [51] E. Runge, E.K.U. Gross, *Phys. Rev. Lett.* 52 (1984) 997-1000.
- [52] M. Petersilka, U.J. Gossmann, E.K.U. Gross, *Phys. Rev. Lett.* 76 (1996) 1212-1215.
- [53] M.J.G. Peach, D.J. Tozer, *The Journal of Physical Chemistry A* 116 (2012) 9783-9789.
- [54] G.A. Crosby, J.N. Demas, *The Journal of Physical Chemistry* 75 (1971) 991-1024.
- [55] C. Würth, M. Grabolle, J. Pauli, M. Spieles, U. Resch-Genger, *Nature Protocols* 8 (2013) 1535-1550.
- [56] L.D. Ramos, H.M.d. Cruz, K.P.M. Frin, *Photochemical & Photobiological Sciences* 16 (2017) 459-466.
- [57] R.M. Spada, M. Cepeda-Plaza, M.L. Gómez, G. Günther, P. Jaque, N. Pizarro, R.E. Palacios, A. Vega, *Journal of Physical Chemistry C* 119 (2015) 10148-10159.
- [58] T. Sainuddin, J. McCain, M. Pinto, H. Yin, J. Gibson, M. Hetu, S.A. McFarland, *Inorg. Chem.* 55 (2016) 83-95.
- [59] M.K. Itokazu, A.S. Polo, D.L.A. de Faria, C.A. Bignozzi, N.Y.M. Iha, *Inorg. Chim. Acta* 313 (2001) 149-155.

- [60] D.M. Dattelbaum, R.L. Martin, J.R. Schoonover, T.J. Meyer, *J. Phys. Chem. A* 108 (2004) 3518-3526.
- [61] M.R. Gonçalves, K.P.M. Frin, *Polyhedron* 132 (2017) 20-27.
- [62] X. Li, D. Zhang, G. Lu, G. Xiao, H. Chi, Y. Dong, Z. Zhang, Z. Hu, *J. Photochem. Photobiol., A* 241 (2012) 1-7.
- [63] P. Larkin, *Infrared and Raman Spectroscopy: Principles and Spectral Interpretation*, Elsevier, 2011.
- [64] R.-R. Ye, C.-P. Tan, M.-H. Chen, L. Hao, L.-N. Ji, Z.-W. Mao, *Chem. Eur. J.* 22 (2016) 7800-7809.
- [65] G.T.S.T. da Silva, F.S. Michels, R.G. Silveira, A.R.L. Caires, G.A. Casagrande, *J. Mol. Struct.* 1185 (2019) 21-26.
- [66] K.K.-W. Lo, K.H.-K. Tsang, K.-S. Sze, *Inorg. Chem.* 45 (2006) 1714-1722.
- [67] J.V. Caspar, T.J. Meyer, *The Journal of Physical Chemistry* 87 (1983) 952-957.